

## Chapter 5: Homophilic interaction of CD150 (SLAM)

### 5.1 Introduction

CD150 is the only member of the CD2 subset for which a homophilic interaction of possible physiological relevance has been observed. Initial reports suggested that the affinity of CD150 for itself may be extremely high compared to other cell surface interactions ( $K_d \sim 0.1 \text{ nM}$ , (Punnonen et al. 1997)). However, if this were the case, the association of cells expressing CD150 would be effectively irreversible and such leukocytes would be unable to interact serially with multiple cells. Interest in CD150 (SLAM) began when it was identified as the antigen recognised by antibodies that could activate CD4<sup>+</sup> T-cells (Cocks et al. 1995) and later because of its differential effects on Th1 and Th2 cells (Castro et al. 1999). CD150 is also of interest because it associates with the signalling molecule SAP, mutations in which cause X-linked lymphoproliferative disorder (Sayos et al. 1998). The current view is that it is a self-ligand involved in bi-directional signalling between B and T cells (Punnonen et al. 1997). However, the extremely high affinity measured for the interaction casts doubt on this hypothesis.

An investigation of the self association of CD150 was undertaken, to test whether this interaction could be detected by alternative methods and whether the reported high affinity was correct. In addition, if such self-association is detected, its properties should shed light on the binding of the putative homophilic ancestor of the CD2 subset. The analytical ultracentrifugation studies described here were undertaken in parallel with SPR studies on the same protein. This work was done by N. Mavaddat and colleagues using a previously untested theoretical framework for analysing weak homophilic interactions and, therefore, required independent confirmation. These SPR studies estimated the  $K_d$  of self-association at 37°C to be approximately 200  $\mu\text{M}$  - an affinity at the extreme low end of the range of affinities previously seen for weak cell surface interactions (Mavaddat et al. 2000).

## **5.2 Materials and Methods**

### **5.2.1 Production of soluble CD150**

The CD150 construct was produced by J. Fennelly and P. Atkinson. A DNA construct encoding the extracellular region of CD150 attached to a BirA recognition site and a six histidine tag was produced in the vector pEE14 as for the wild-type CD150 used for crystallisation (which lacked the BirA site, see chapter 3). This construct was transfected into CHO K1 cells using calcium phosphate as for the CD244 constructs described in chapter 2. Production of the protein in cell factories, purification using a nickel column, size-exclusion gel chromatography and removal of the histidine tag with carboxypeptidase A were carried out as described for other protein constructs (chapters 2 and 3). The soluble CD150 protein produced was named sCD150.

### **5.2.2 Analytical ultra-centrifugation: sedimentation equilibrium method**

Analytical Ultracentrifugation (AUC) follows the absorbance of proteins in solution under centrifugal forces. The protein is centrifuged in a rotor that allows the absorbance of the sample to be measured at regular points along its radius. The movement of the protein down the cell under centrifugal force can therefore be followed. The motion of the protein depends on the centrifugal force applied, its mass and the resistance of the solution, which depends on the shape of the protein. Thus, the mass of protein species in solution can be calculated and its shape modelled from the absorbance data collected. This method can therefore be used to determine whether proteins associate with each other, as this will affect the apparent mass of the species in solution, and by varying the concentration of protein used, the dissociation constant can be calculated.

Because the centrifugal force is eventually countered by diffusion away from the highly concentrated solution at the base of the cell, if samples are centrifuged at slow speeds for

sufficient time, thermodynamic equilibrium is reached. The absorbance of the solution at different radii along the centrifugal cell at equilibrium depends on the partial specific volume and average molecular mass of the protein in solution. If the protein associates into oligomers or multimers, the apparent molecular mass will be dependent on the concentration of the protein. This method of analysis (sedimentation equilibrium) was attempted for sCD150.

Various concentrations of sCD150 were centrifuged at 10,000 rpm for 16 hours in a Beckman Optima XL-A analytical ultracentrifuge at 37°C. 12mm pathlength, Yphantis-type centrepieces were used, with each one containing three samples and three corresponding channels of pure solvent - allowing the subtraction of solvent absorbance. The absorbance of 298nm wavelength light was measured at multiple points along the radius of the cell (without stopping the centrifuge) and then the samples were centrifuged for a further three hours. If absorbance readings remained constant after these three hours, equilibrium was said to have been reached. Specific absorbance (i.e. after subtraction of solvent absorbance) was plotted against radius and the data were fitted using the equation:

$$A(r) = A(r_F) \exp \left[ M_{w,app} \frac{(1 - \bar{v}\rho)\omega^2}{2RT} (r^2 - r_F^2) \right] + E$$

Where  $A(r)$  is the absorbance at radius  $r$  in cm,  $A(r_F)$  is the absorbance at the reference radius  $r_F$ ,  $M_{w,app}$  is the apparent whole cell average molecular weight,  $\bar{v}$  is the partial specific volume in ml/g,  $\rho$  is the solvent density in g/ml,  $\omega$  is the angular velocity of the rotor in rad/s,  $R$  is the gas constant,  $T$  is the absolute temperature, and  $E$  is the baseline offset.

The baseline offset was calculated by pelleting the sample at 40,000 rpm after equilibrium and measuring the background absorbance of protein-depleted solvent. If the equation above gave a good fit to the absorbance data, it could then be used to calculate the apparent molecular weight ( $M_{w,app}$ ) of the solute at each protein concentration. Plotting  $M_{w,app}$  against

concentration and fitting with the equation below should then enable the calculation of a  $K_d$  for self-association.

$$M_{w,app} = \frac{(n-1)M_1c}{K_d + c} + M_1$$

Where  $n$  is the association state of the complex formed (e.g. 2 for a dimer),  $M_1$  is the molecular weight of the monomer,  $c$  is the protein concentration and  $K_d$  is the dissociation constant of the interaction.

### 5.2.3 Analytical ultra-centrifugation: sedimentation velocity method

An alternative method to measuring absorbance at thermodynamic equilibrium is to follow the movement of the protein down the cell during centrifugation. This is termed velocity AUC. Various concentrations of sCD150 were centrifuged at 40,000 rpm in a Beckman Optima XL-A analytical ultracentrifuge at 37°C, using double sector centrepieces with pure solvent (HBS) in the opposing sector to control for solvent absorbance. Pathlengths of 3 or 12mm were used depending on protein concentration. The sedimentation of the boundary between depleted solvent and protein solution was followed using incident light at wavelengths of 254, 278, 298 or 305nm. At high protein concentrations, a schlieren signal was observed in the absorbance scans. This has previously been reported and was shown to be a function of the precise configuration of the AUC monochromator (Coelfen and Harding 1995), which varies between instruments. The schlieren signal was controlled for by collecting data at different wavelengths and resulted in an additional peak in the  $g(s^*)_t$  profiles (see below) at low  $s^*$  when using affected wavelengths. The schlieren contribution was allowed for at the stage of fitting these  $g(s^*)_t$  profiles.

The data was analysed using the time derivative ( $g(s^*)_t$ ) method (Stafford 1992).  $g(s^*)_t$  (in arbitrary units) is the distribution of apparent sedimentation coefficients ( $s^*$ ) at the boundary calculated from the time derivative of a series of boundary traces using the equation:

$$g(s^*)_t = \left( \frac{d\{c(r,t)/c_0\}}{dt} \right) \left( \frac{\omega^2 t^2}{\ln(r_m/r)} \right) \left( \frac{r}{r_m} \right)^2$$

Where  $c$  is the concentration in absorbance units,  $r$  is the radial distance from the centre of the rotor in cm,  $t$  is the time since the start of the experiment in seconds,  $c_0$  is the concentration at time zero,  $\omega$  is the angular velocity of the rotor in rads/s, and  $r_m$  is the radius at the meniscus in cm. The calculated  $g(s^*)_t$  profile was fitted with single or multiple Gaussian distributions using the ProFit (Quantun Software, CA) curve-fitting software package. Residuals were calculated to judge the quality of the fit generated. The simplest (lowest order) fit that did not result in any systematic variation in the residuals was used.

The mid-point of each Gaussian distribution detected corresponds to the apparent sedimentation coefficient ( $s^*$ ) of one protein species in the solution. The  $s^*$  values for each species, determined by fitting the  $g(s^*)_t$  profiles, were plotted against protein concentration, extrapolated to zero concentration and corrected for the effects of solvent density and viscosity and the temperature at which the experiment was performed (using Sednterp (Laue 1992)) to yield values of  $s_{20,w}^0$ , the sedimentation coefficient in water at 293K (20°C) at infinite dilution.

The area enclosed by each Gaussian distribution corresponds to the amount of that species present in the solution (in absorbance units). The ratio of these amounts at different sCD150 concentrations allows the calculation of association/dissociation constants. The ratio of areas (R) corresponds to the ratio of bound sCD150 to free sCD150 and therefore equals one when the protein concentration equals the dissociation constant ( $K_d$ ).

## 5.2.4 Shape modelling

The  $s_{20,w}^0$  value derived above was used to calculate the frictional ratio ( $f/f_0$ ) displayed by each species observed, using the following equation (Carrasco et al. 1999):

$$\frac{f}{f_0} = \frac{M(1 - \bar{v}\rho_0)}{N_A 6\pi\eta_0 s_{20,w}^0 \left( \frac{3\bar{v}M}{4\pi N_A} \right)^{\frac{1}{3}}}$$

Where  $M$  is the mass of the species (in g/mol),  $\bar{v}$  is its partial specific volume,  $\rho_0$  and  $\eta_0$  are the density and viscosity of water respectively and  $N_A$  is Avogadro's number. This ratio was then used to calculate the experimental Perrin function ( $P_{\text{exp}}$ ), which describes the axial ratio of the species, and the anhydrous sedimentation coefficient ( $s_0$ ) of the species if it existed at various levels of hydration ( $\delta_{\text{app}}$  is the apparent hydration in g of H<sub>2</sub>O per g of protein):

$$P_{\text{exp}} = \frac{f}{f_0} \left[ 1 + \left( \frac{\delta_{\text{app}}}{\bar{v}\rho_0} \right) \right]^{\frac{1}{3}} \quad \text{and} \quad s_0 = s_{20,w}^0 \left[ 1 + \left( \frac{\delta_{\text{app}}}{\bar{v}\rho_0} \right) \right]^{\frac{1}{3}}$$

Theoretical values for the Perrin function ( $P_{\text{calc}}$ ) and anhydrous sedimentation coefficient were calculated from hydrodynamic bead models of sCD150 monomers and dimers using the program SOLPRO (Garcia de la Torre et al. 1999). These bead models were calculated from model atomic structures using the program AtoB (Byron 1997). The model atomic structure used for the sCD150 monomer was derived from the crystal structure of rat CD2 (Jones, E. Y. et al. 1992) by adding eight octasaccharides chains at the positions in rat CD2 that align with the glycosylation sequons in the CD150 protein sequence. These octasaccharides represent the average N-linked carbohydrate structure added by CHO cells (Ashford et al. 1993), and were modelled in random orientations. The model for the sCD150 homodimer was created by orienting two copies of this monomer model by superposition of their V-set IgSF domains on those of CD2 and CD58 in the crystal structure of the CD2-CD58 complex (Wang et al. 1999) using the program SHP (Stuart et al. 1979).

## 5.3 Results and discussion:

### 5.3.1 Observation of CD150 homophilic interaction

Initially, various concentrations of a soluble CD150 construct (sCD150) were analysed by sedimentation equilibrium AUC. Unfortunately, the variation of absorbance with radius observed in this equilibrium state could not be accurately fitted with the appropriate equation to determine the average molecular mass in the cell (see methods). The protein solution apparently behaved non-ideally at the concentrations of sCD150 used. The behaviour of low concentrations of sCD150 could be fitted, but no variation was seen in the average molecular mass (data not shown) - as expected unless extremely high affinity self-association occurs. An alternative method that does not require modelling of protein behaviour is velocity AUC (see methods) and this technique was used to analyse sCD150 self-association successfully.

*Figure 5.1a* shows a series of absorbance scans for a single sCD150 concentration, collected at regular intervals during centrifugation. Changes in the location and shape of the boundary between protein-depleted solvent and remaining sample were analysed via the time-derivative of pairs of scans to yield the function  $g(s^*)$  (see methods), which gives the distribution of apparent sedimentation coefficients at the boundary (*Fig. 5.1b*, bottom panel) (Stafford 1992). A single, monodisperse species will display a normal Gaussian distribution of  $s^*$  due to the symmetrical nature of its boundary. Systematically varying residuals indicate that the distribution does not fit a single Gaussian peak (*Fig. 5.1b*, top panel) whereas a good fit is observed for a two species model (*Fig. 5.1b*, middle panel). Higher order models did not give a significantly better fit to the data and on iteration, they approximate to the two species model. Thus, two forms of sCD150 are present in the solution.

The mid-points of the two Gaussian distributions represent the sedimentation coefficients for the two species - for the concentration shown in *Figure 5.1a-b*, these are 5.48 S and 6.2 S.

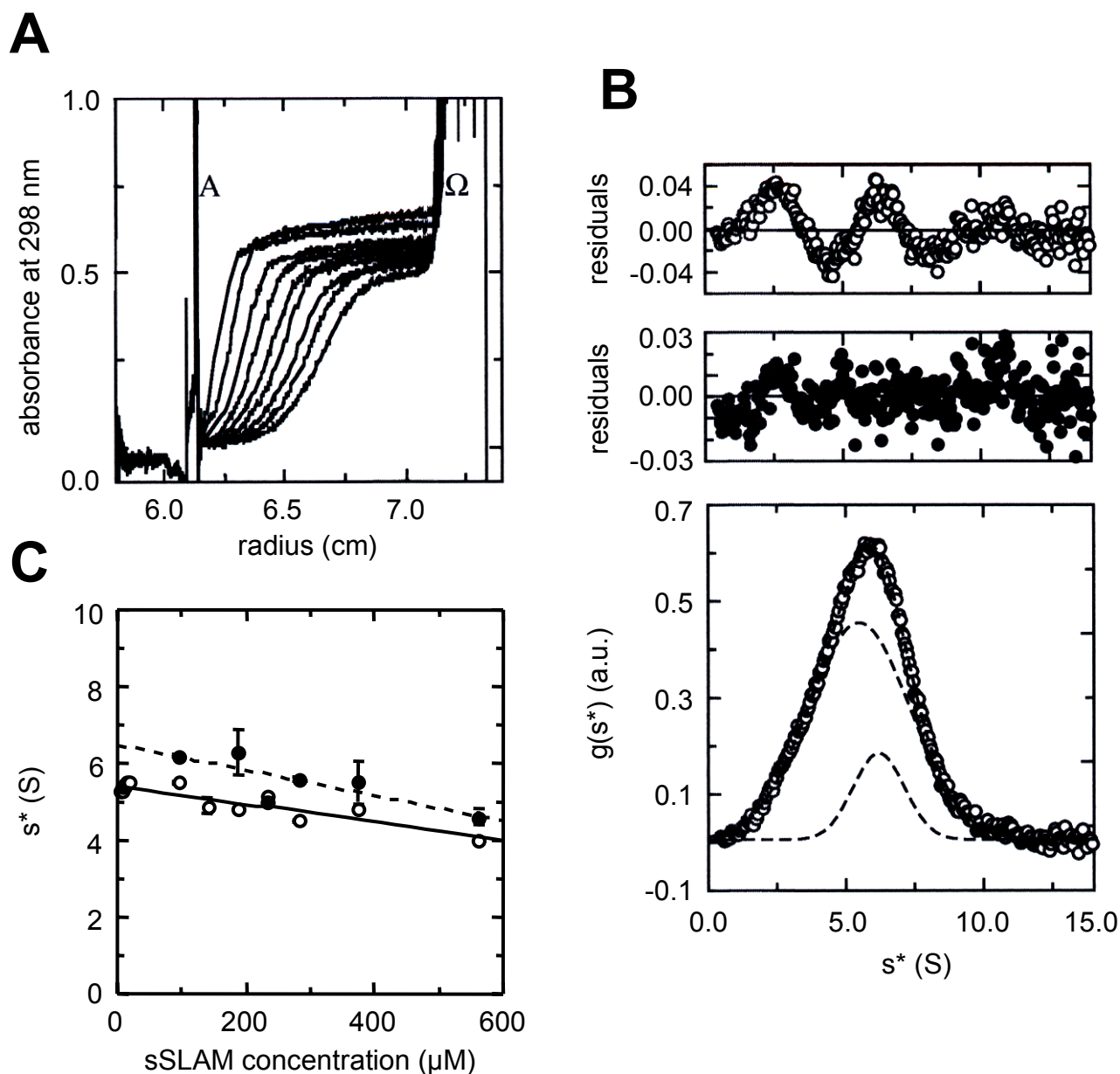


**Figure 5.1: Analytical ultracentrifugation of sCD150 detects self-association.**

**A.** Absorbance scans at 298nm for sCD150 at ~3mg/ml collected at intervals of 15 minutes are shown with the sample moving from left to right. Traces mark the migration of sCD150 along the centrifugal cell from the sample meniscus (A) to the cell bottom ( $\Omega$ ).

**B.** The *bottom panel* shows the  $g(s^*)$  distribution for sCD150 at ~3mg/ml at 37°C ( $\circ$ ). The data is fitted with the sum of two Gaussian distributions (dashed lines), representing species with  $s^*$  of  $5.48 \pm 0.02$  S and  $6.20 \pm 0.02$  S respectively. The residuals ( $\bullet$ ) for this fit are shown in the *middle panel*. The residuals ( $\circ$ ) of a single species fit (i.e. with the data fitted to a single Gaussian distribution) are shown in the *top panel* for comparison.

**C.** Values of  $s^*$  for species 1 ( $\circ$ ) and species 2 ( $\bullet$ ) are plotted against sCD150 concentration. The error bars represent the standard errors on the Gaussian fit midpoints. Linear fitting of the data (solid line for species 1, dashed line for species 2) and extrapolation to zero concentration yields  $s^{*0}$  ( $s^*$  at infinite dilution) values of  $5.42 \pm 0.07$  S and  $6.73 \pm 0.20$  S, which were then corrected for effects of solvent and temperature to yield  $s_{20,w}^0$  values of 3.8 and 4.7 respectively (see text).

The effects of buffer density and viscosity and the experimental temperature were corrected for and, to account for the diffusion limiting effects of high protein concentration, the sedimentation coefficients were measured at a series of concentrations (**Fig. 5.1c**).

Extrapolation to infinite dilution yielded an  $s_{20,w}^0$  of  $3.8 \pm 0.1$  S for the smaller species and  $4.7 \pm 0.2$  S for the larger species. The areas of the two Gaussian distributions of  $g(s^*)$  found in the sample are proportional to the amount of each species present. The ratio of these areas was found to be highly concentration dependent; ruling out the possibility that the two species are different glycoforms of sCD150 or that one is an impurity - in either of these cases, the ratio of the areas would remain constant with increasing concentration. Thus, the two species are two states of an interacting system - in this case monomeric and dimeric sCD150.

### **5.3.2 Estimation of the affinity of CD150 for itself**

By plotting the ratio of the areas of the two Gaussian distributions against the total sCD150 concentration in the sample (**Fig. 5.2**), we can estimate the  $K_d$  of the CD150-CD150 interaction. An exponential fit of this data allows us to read the concentration of sCD150 at which the ratio is 1 (when  $[sCD150]_{bound} = [sCD150]_{free}$ ) and thus estimate the  $K_d$ . This method yields a value of  $\sim 200\mu M$  (**Fig. 5.2a**) in agreement with SPR data (Mavaddat et al. 2000). However, a more rigorous approach is to derive the ratio of free to bound sCD150,  $R$ , in terms of  $K_a$  ( $1/K_d$ ). Although the data does not fit such an exact model, plotting theoretical  $R$  at various values of  $K_d$  shows that the data fit a  $K_d$  in the range  $100\mu M - 1mM$  (**Fig. 5.2b**). From this result, it is clear that CD150 homodimerisation occurs with an affinity *weaker* than that of most cell surface interactions studied, rather than one that is much greater, as initially reported (Punnonen et al. 1997).

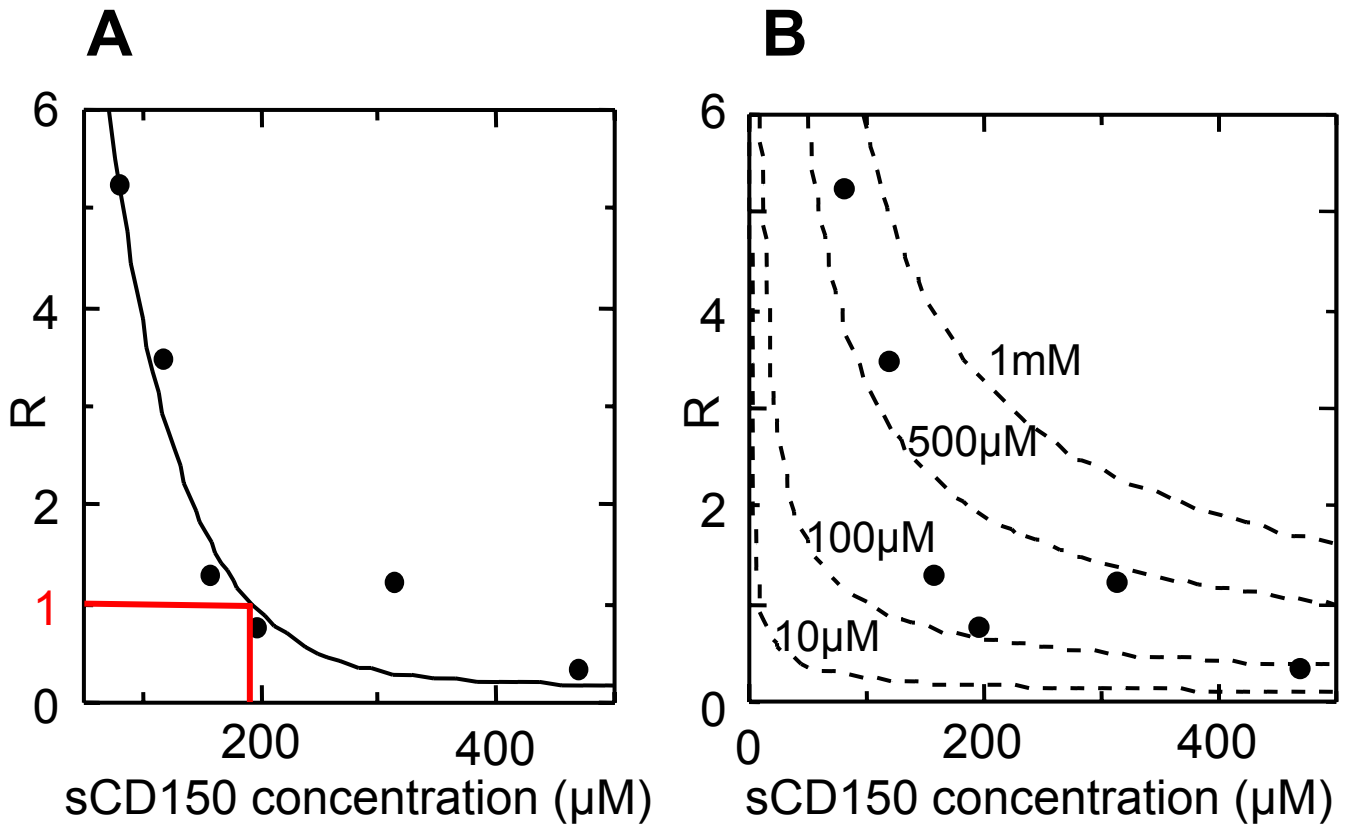


**Figure 5.2: Estimation of the affinity of CD150 self-association by AUC.**

The observed ratio ( $R$ ) of the areas of the two Gaussian distributions seen in the  $g(s^*)_t$  profiles of sCD150 (see **Fig. 5.1**) is calculated and plotted against total sCD150 concentration. The relationship between  $R$  and the molar concentrations of the sCD150 species is as follows:

$$R = \frac{A_{monomer}^{298}}{A_{dimer}^{298}} = \frac{[Monomer]}{2[Dimer]} = \frac{[sCD150]_{free}}{[sCD150]_{bound}}$$

**A.** The data is fitted with a simple exponential decay curve (solid line). The  $K_d$  is the concentration at which  $R = 1$  (half maximal binding), therefore by this fit  $K_d \sim 200\mu\text{M}$ .

**B.** Using the additional relationships,

$$K_a = \frac{[Dimer]}{[Monomer]^2} \quad \text{and} \quad S_T = [Monomer] + 2[Dimer]$$

(where  $S_T$  is the total sCD150 concentration)

$R$  can be derived in terms of  $S_T$  and  $K_a$ :

$$R = \frac{\sqrt{1 + 8K_a S_T} - 1}{4K_a S_T - \sqrt{1 + 8K_a S_T} + 1}$$

The dashed lines illustrate the expected dependence of  $R$  on total sCD150 concentration for given values of  $K_d$  (from  $10\mu\text{M}$  to  $1\text{mM}$ ) calculated using this equation. According to this analysis, the  $K_d$  for sCD150 self-association is between  $100\mu\text{M}$  and  $1\text{mM}$ .

### 5.3.3 Estimation of the shape of the CD150-CD150 complex

The behaviour of a species during centrifugation depends on both its mass and its shape as these properties affect its diffusion coefficient. The experimental Perrin function ( $P_{\text{exp}}$ ) is a size independent parameter describing the degree of elongation of a species (i.e. the ratio of its length to its width). The values of  $s_{20,w}^0$  calculated for the sCD150 monomer and dimer were used to determine  $P_{\text{exp}}$  and  $s_0$  (dehydrated sedimentation coefficient at infinite dilution) for the two species at a range of possible hydration levels (**Table 5.1**). Theoretical values of  $P_{\text{calc}}$  and  $s_0$  were then calculated for hydrodynamic bead models of sCD150 monomers (**Fig. 5.3a**). These models were made from the structure of rat CD2 (Jones, E. Y. et al. 1992), with standard CHO cell carbohydrates added to residues aligning with the glycosylation sequons of CD150 (see methods).  $P_{\text{calc}}$  and  $s_0$  values were also calculated for a model of the sCD150 dimer created using the structure of the human CD2-CD58 complex (Wang et al. 1999) to align two copies of the monomer model (**Fig. 5.3b**). The calculated values of  $P_{\text{calc}}$  and  $s_0$  for the monomer were 1.47 and 4.07 S and those for the dimer were 1.6 and 5.08 S, in reasonable agreement with the experimental values (**Table 5.1**). Although our modelling is likely to be inexact, in that it does not allow for any inherent flexibility such as that of the carbohydrate moieties, this analysis strongly suggests that the dimer has an end-to-end topology, similar to that of CD2 with its ligands, rather than a side-to-side topology or a random topology resulting from non-specific aggregation effects. In either of these cases, aggregation would cause  $P_{\text{exp}}$  to either remain unchanged or fall and the sedimentation coefficient to nearly double; for example, side-to-side dimerisation of sB7-1 (Ikemizu et al. 2000) increases  $s_0$  from 2.58 S to 4.08 S but only changes  $P_{\text{exp}}$  from 1.27 to 1.28.

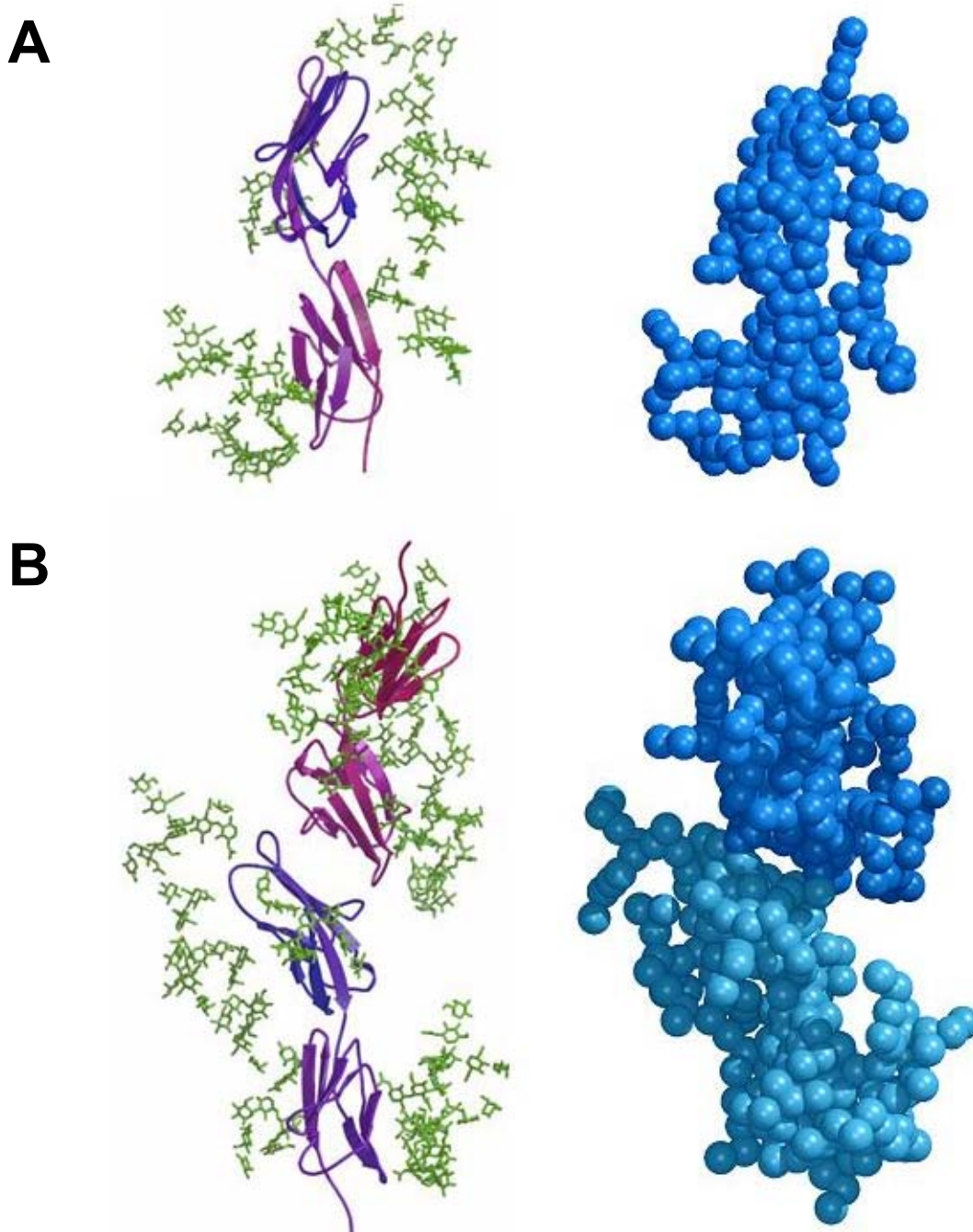


**Figure 5.3: Molecular modelling of sCD150 monomer and dimer structures.**

**A.** The structure of soluble rat CD2 (Jones, E. Y. et al. 1992) is shown (left) with modelled N-linked oligosaccharides (green) attached in random orientations at positions likely to correspond to CD150 glycosylation sequons according to sequence alignments (data not shown). The corresponding bead model, constructed using AtoB (Byron 1997), is shown in the same orientation (right).

**B.** A model of the sCD150 homodimer, constructed by superimposing the monomer model (in **A**) on the CD2 and CD58 domain structures solved in complex (Wang et al. 1999) is shown (left). The corresponding bead model is again shown (right).

These bead models were used to calculate the theoretical hydrodynamic parameters for the sCD150 monomer and homodimer described in the text.

The images were generated using BOBSCRIPT (Kraulis 1991; Esnouf 1997) and rendered with Raster3D (Merritt and Murphy 1994).

Apparent hydration ( $\delta_{app}$ , g(H <sub>2</sub> O)/g(protein))	Species 1 ( $s_{20,w}^0 = 3.8$ S)		Species 2 ( $s_{20,w}^0 = 4.7$ S)	
	$P_{exp}$	$s_0$ (S)	$P_{exp}$	$s_0$ (S)
0.1	1.322	4.0	1.708	4.9
0.2	1.271	4.1	1.643	5.1
0.3	1.227	4.3	1.586	5.3
0.4	1.189	4.4	1.536	5.5
0.5	1.155	4.5	1.492	5.6

**Table 5.1: Experimental shape statistics for the two sCD150 species observed by AUC.** Experimental Perrin ratios ( $P_{exp}$ ) and anhydrous sedimentation coefficients ( $s_0$ ) calculated for the two species observed in the  $g(s^*)_t$  profiles at a range of apparent hydrations ( $\delta_{app}$ ).

Values were calculated using the following equations,

$$P_{exp} = \frac{f}{f_0} \left[ 1 + \left( \frac{\delta_{app}}{\bar{v}\rho_0} \right) \right]^{\frac{1}{3}} \quad \text{and} \quad s_0 = s_{20,w}^0 \left[ 1 + \left( \frac{\delta_{app}}{\bar{v}\rho_0} \right) \right]^{\frac{1}{3}}$$

Where  $f/f_0$  is the frictional ratio calculated using the equation:

$$\frac{f}{f_0} = \frac{M(1 - \bar{v}\rho_0)}{N_A 6\pi\eta_0 s_{20,w}^0 \left( \frac{3\bar{v}M}{4\pi N_A} \right)^{\frac{1}{3}}}$$

$M$  is the mass of the species (in g/mol),  $\bar{v}$  is its partial specific volume and  $s_{20,w}^0$  is its experimentally determined, apparent sedimentation coefficient at infinite dilution corrected for solvent and temperature effects.  $\rho_0$  and  $\eta_0$  are the density and viscosity of water respectively and  $N_A$  is Avogadro's number.

### 5.3.4 Is there another CD150 ligand?

Both this study and SPR studies (Mavaddat et al. 2000) demonstrate that the affinity of CD150 homodimerisation is extremely weak - comparable to the interaction of CD8 with MHC class I molecules ( $K_d = 200-300\mu\text{M}$  (Wyer et al. 1999)). It is unclear whether such an affinity is sufficient for CD150 on one cell to interact with that on another cell *in vivo*. The relevant parameter to assess such a possibility is the two dimensional affinity. For the rat CD2-CD48 interaction ( $K_d$  in solution =  $80\mu\text{M}$ ), the two dimensional affinity barely supports contact between a cell and a planar bilayer containing the molecules at physiological levels (Dustin et al. 1997). Therefore, weaker interactions such as CD150 homodimerisation may be unable to occur between two cells. In line with this, it has been argued that the CD8-MHC class I interaction occurs only when stabilised by additional interactions with a TCR (bound by both CD8 and the MHC molecule) (Wyer et al. 1999). It is possible that CD150 self-association between cells may occur if CD150 was expressed at extremely high levels or if the interaction was stabilised by other molecules (as in the case of CD8-MHC class I). However, it is perhaps more likely that there is another, true CD150 ligand and that this homodimerisation may simply be evidence of the evolution of members of the CD2 family from a homophilic ancestor. A similar, non-physiological, homophilic interaction has been reported for CD2, although it is much weaker ( $K_d \sim 3-6\text{mM}$  (Pfuhl et al. 1999)).